Research on Thermal-Mechanical Properties of GaN Power Module Based on QFN Package by Using Nano Copper/Silver Sinter Paste

Li, Shizhen; Liu, Xu; Fan, Jiajie; Tan, Chunjian; Wang, Shaogang ; Xie, Bin ; Ye, Huaiyu

DOI
10.1109/ICEPT56209.2022.9873399

Publication date
2022

Document Version
Final published version

Published in
Proceedings of the 2022 23rd International Conference on Electronic Packaging Technology (ICEPT)

Research on Thermal-Mechanical Properties of GaN Power Module Based on QFN Package by Using Nano Copper/Silver Sinter Paste

1st Shizhen Li
School of Microelectronics, Southern University of Science and Technology
Shenzhen, China
lisz@mail.sustech.edu.cn

2nd Xu Liu
Electrical Engineering, Mathematics and Computer Science, Delft University of Technology
Delft, The Netherlands
X.liu-12@tudelft.nl

3rd Jiajie Fan
Academy for Engineering&Technology, Fudan University
Shanghai, China
jiajie_fan@fudan.edu.cn

4th Jing Jiang
Academy for Engineering&Technology, Fudan University
Shanghai, China
19110860049@fudan.edu.cn

5th Chunjian Tan
Electrical Engineering, Mathematics and Computer Science, Delft University of Technology
Delft, The Netherlands
c.tan@tudelft.nl

6th Shaogang Wang
Electrical Engineering, Mathematics and Computer Science, Delft University of Technology
Delft, The Netherlands
S.Wang-10@tudelft.nl

7th Bin Xie
Hong Kong Applied Science and Technology Research Institute
Hong Kong, China
bxie@astri.org

8th Huaiyu Ye*
Southern University of Science and Technology
Shenzhen,China
yehy@sustech.edu.cn

2022 23rd International Conference on Electronic Packaging Technology (ICEPT) | 978-1-6654-9905-7/22/$31.00 ©2022 IEEE | DOI: 10.1109/ICEPT56209.2022.9873399

***Abstract*—The wide-bandgap semiconductors represented by GaN have a broad application prospect because of their high service temperature and high switch frequency. Quad-Flat-No-Lead (QFN) Package is currently one of the mainstream packaging methods due to its low cost and high efficiency. However, the low reliability of QFN used in GaN devices is still a crucial problem caused by elevated temperatures and the thermal stress induced by the mismatch of coefficient of thermal expansion (CTE). Therefore, it is necessary to control the temperature inner the package and increase the mechanical property of the bonding layer. In this paper, the finite element method (FEM) with thermal-mechanical coupling is performed to optimize the reliability of the bonding layer by adopting sinter nano Cu and silver. Based on the conventional QFN package module, we tried to add different metallization on the bonding surface to decrease the influence of CTE mismatch. We should note that the Anand viscoplastic model was used in the materials of Sintered Ag and lead-free solder paste presented by SAC305, which were the most commonly used in die-attachment. The results showed that the utilization of nano copper/silver paste could hardly facilitate thermal performance although sintered Ag had excellent thermal conductivity. Since the Anand modules of Ag and SAC305 were different, there were some impacts on the stress distribution and deformation. During the bonding process, a large thermal stress generated between die-attachment layer and Package or the PCB. The die-attachment layer formed by nano Ag paste suffered the smaller thermal stress because its CTE is comparable to that of thermal pad. In terms of sintered Ag, the bonding layer generated more elastic strain. As the deformation recovered to initial stage, the stress decreased because of the elastic strain. And we also found that the Ag metallization could decreased the maximum stress of model at heating stage. But Ag metallization suffered larger thermal stress as the temperature decreased. The selection of connection materials and metallization are a crucial part of design the structure of electronic package. And this paper could provide a reference for optimize the package structure to further improve their reliability in future works.**

Keywords—GaN, QFN, simulation, sintered Ag, thermal stress

I. Introduction

As an important part of electrical equipment, power devices carry the functions of inverter, control, and current handling [1]–[3]. At present, the more common commercial power devices on the market are mainly developed based on silicon (Si). Due to the limitation of material characteristics, the power density of silicon based semiconductor is up to 200W/cm2, and the service temperature is up to 175℃ [4], [5]. With the development of power electronics technology, wide bandgap semiconductors represented by SiC and GaN have been widely studied in power device packaging and modules[6]. Compared with silicon-based semiconductors, wide bandgap semiconductors have the advantages of high voltage drop, high switching speed, high power density and high service temperature, and are widely used in high-power devices. Therefore, power device packages and modules often need to serve in high frequency, high voltage and high temperature environment, which poses a higher challenge to the reliability of chip packages.

QFN packages are widely used in Surface-Mount-Technology because of their simple structure, low cost and easy operating. The structure of QFN is shown in Figure 1[7]. A QFN packages is mainly composed of chip, plastic encapsulation, IOs, and PCB. Since the working process of QFN generates large amounts of heat, a thermal pad is necessary for QFN to dissipate heat, which could prevent the chip damage because of excessive temperature.

Therefore, a bonding layer is needed to connect thermal pad and PCB. Currently, the main bonding materials used in electronic packaging are the SAC series of brazing materials, nano-copper and nano-silver pastes. However, due to the heat exists in system, the difference of thermal expansion coefficients of materials will generate thermal-stress, which

will result in damaging of package structure. The location where damage occurs is at the connection between the QFN and PCB. Hence, it is necessary to analyse the thermal

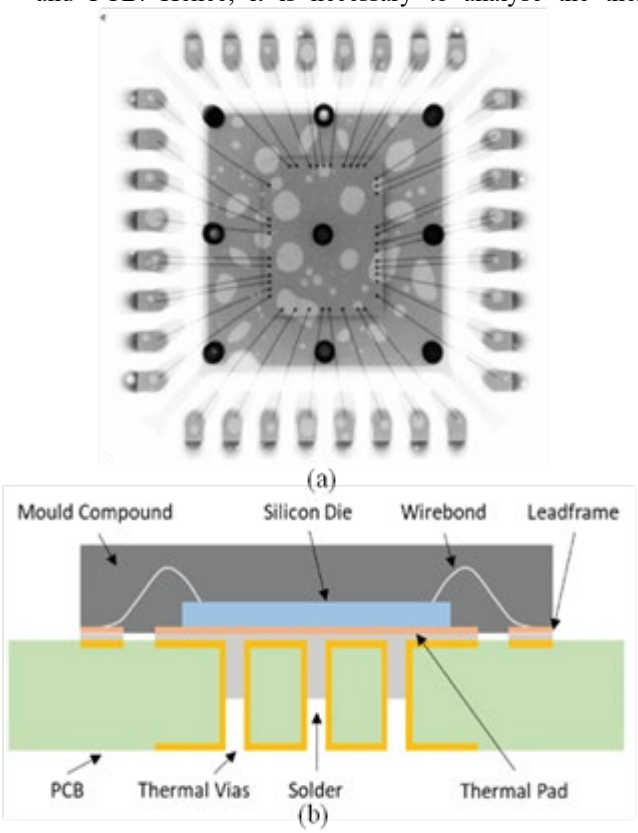

Fig. 1 (a) The inner structure of QFN package system (b) QFN package soldered on a PCB with Thermal vias stresses for the connection layer.

Table 1 The details of model parameters

Model parameter setting (mm)	
GaN chip	3.5*3.5*0.5
QFN pakage	6*6*1
Thickness of top encapsulation	0.25
QFN thermal pad	5*5*0.25
bonding layer	5*5*0.2
metallization	5*5*0.1
PCB	18*18*1.5
Radius of Via	0.3
Thickness of Via	0.015
IO	32

In this paper, we will investigate the effects of bonding materials on the thermal stress of QFN packages at bonding area. After that, we will analyze effects of PCB metallization on QFN Packages based on previous results. This work could provide the reference for design of QFN Packages' joints.

II. Simulation Method And Model

Finite element method has been widely used in investigate the thermal distribution and stress distribution in electronic industry. Therefore, the simulation will be performed by FEM based on Ansys Mechanical software.

In order to reduce the simulation and analyze difficulty, we made some simplifications to the model. Figure 1 shows that the bonding wire is used to connect the chips and IO. Since in this work we mainly focus on thermal and stress distribution, and the bonding wire generated limited heat during service process, the bonding wire did not include in this model. And due to the symmetry structure, we only build 1/4th of the volume to decrease the simulation time. Two symmetry planes were set to keep the accuracy of simulation.

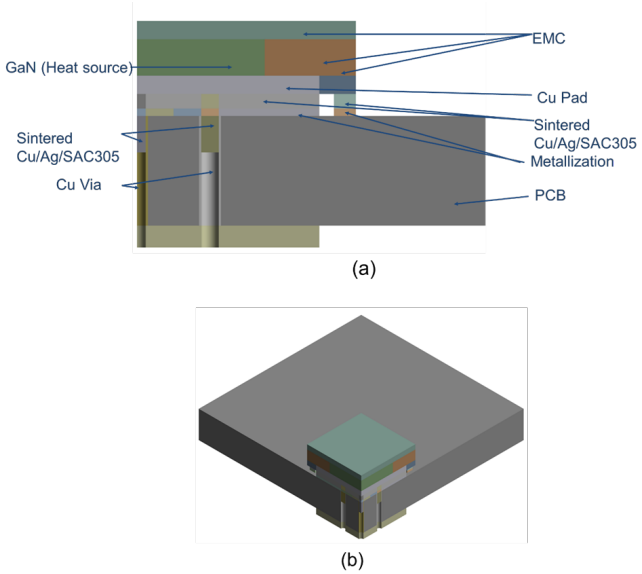

Fig. 3 (a) Implemented model of the QFN (b) The whole structure of model used in this simulation

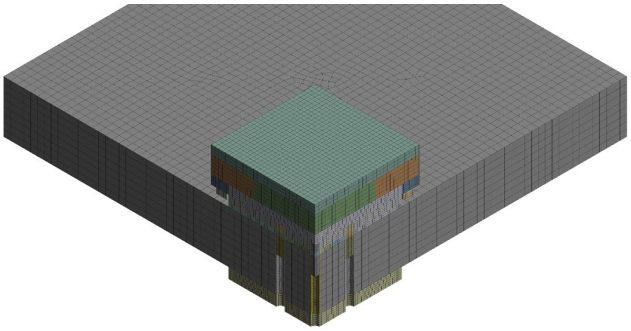

Fig. 2. The 3D view of meshed simulation model

In this model[7], there were 9 via in the center of PCB coated by thin copper film. The QFN package directly connected with PCB by connection layer and metallization layer. Therefore, the joint of this model is a four-layer structure, which were Cu pad, bonded layer, metallization layer and PCB. The details of model parameters were shown in Table 1. And the Figure 2 showed the generated model.

Figure 3 was the mesh structure of model. In this simulation, the quality of mesh was between 0.5-1, which had already exceeded the basic requirements to allow for simulation. The bonded connection settings were used to build the link

Table 2 The basic materials' properties used in this model

Thermal and mechanical property of materials						
Materials	Density (kg m^-3)	Thermal property		Mechanical property		
		Thermal Conductivity (W m^-1 C^-1)	Specific Heat (J kg^-1 C^-1)	Thermal Expansion Coefficient (C^-1)	Young's Modulus (Mpa)	Poisson's Ratio
Ag Bulk	10500	429	235	2.07E-05	6.90E+04	0.37
GaN	6100	110	534	5.60E-06	1.81E+05	0.352
PCB	1900	0.38	1103	1.55E-05	2.46E+04	0.136
EMC	2000	20	1694	6.50E-05	2.50E+04	0.37
Sintered Ag	6294	240	350	1.92E-05	6E+03	0.37
SAC305	7400	57.8	232	2.21E-05	3.60E+04	0.3

between two bulks. The most part of meshes were Hexahedral grides. Only a very limited parts around the via were triangular prism mesh. The range of size of mesh is from 0.05 to 0.5mm, which depended on the size of parts. In order to promise the accuracy of simulation and decrease the calculation cost, we assigned the larger mesh for parts with larges size.

The detail information of materials used in this model were shown in Figure 32 Since we mainly focus on the stress state of bonded layer, the Anand model were used to calculate the stress state of bonded layer, SAC305, sintered Cu and sintered Ag. The Anand parameters of sintered Ag and SAC305 were shown in Table 3. Due to the Anand model of Sintered Cu were derived from previous work, which has not been published, readers could contact corresponding writer to ask for detail Anand model information of sintered Cu.

Table 3 The parameters of Anand model of Sintered Ag and SAC305

Parameters	units	Sintered Ag	SAC[8]
A	1/S	2.537	5.87E+6
Q/R	K	3463.5	7460
ε	-	12	2
m	-	0.20473	0.0942
h0	Mpa	696.06	9350
ŝ	Mpa	168.15	58.3
n	-	0.12348	0.015
a	-	1	1.5
S0	MPa	2.224	57.8

In thermal simulation, we gave a internal heat generation, 0.2W/mm3, to GaN chip. The convection of 2.5E-5W/mm2*K were applied to all the surfaces. The ambient temperature was 20℃. The thermal simulation could be

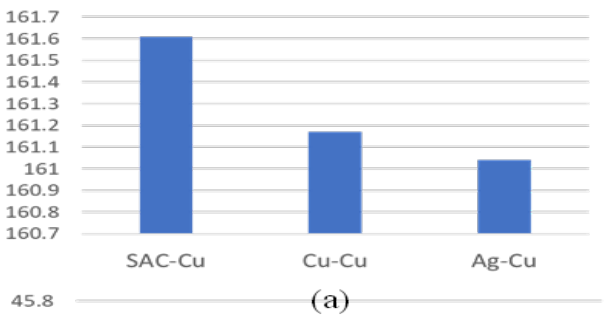

(a)

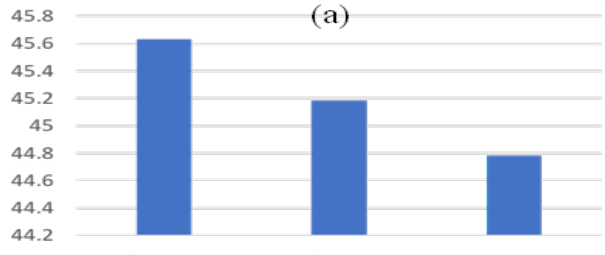

(b)

Fig. 5 The temperature distribution of the whole system at (a) 300s and (b) 390s

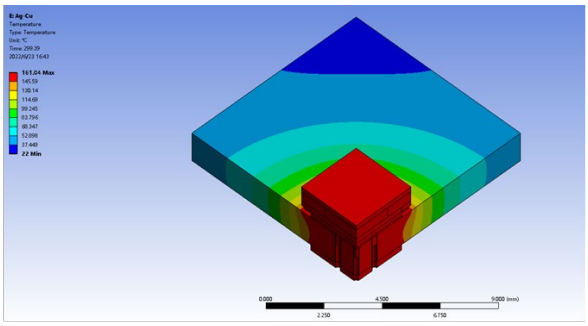

(a)

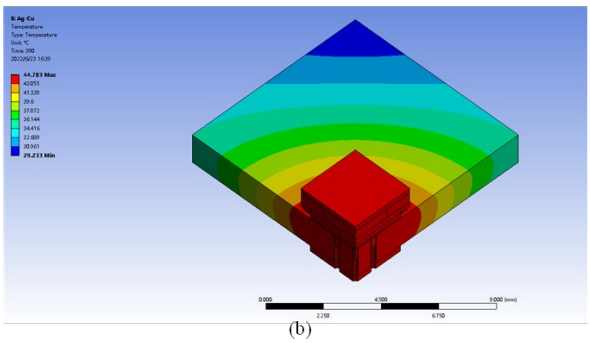

(b)

Fig. 4 Temperature distribution of QFN Package model at (a) 300s (b) 390s

divided into four stages. In first stage, from 0 to 30s, the internal heat generation rose from 0 to 0.2 W. In second stage, the system heated with 0.2W/mm3 from 30 to 300 s. After that, in third stage, the heat generation decreased to 0 uniformly. And the last stage, from 330-390s, was the cooling stage. In mechanical simulation, we imported the temperature results to the initial conditions. The weak spring was open to prevent the rigid body displacement because of the unfix setting. This simulation contained 4 types of strategy, SAC305, sintered Cu and sintered Ag connected with Cu metallization and sintered Cu connected with Ag metallization (SAC-Cu, Cu-Cu, Ag-Cu and Cu-Ag).

III. Results and Discussion

A. Thermal Analysis

Figure 4(a) and (b) showed the thermal distribution of the whole system. At 300s, the temperature reached highest. The maximum temperature is 161.04℃. We could observe that the heat was mainly concentrated at the QFN package. The temperature difference at vertical direction is not significant. At the end of simulation, the highest temperature in system had decreased to 44.783℃. This results was based on the model which bonding layer was sintered Ag. Since the purpose of this simulation is to investigate the effects of

bonding layer type, the max temperatures results at 300s and 390 ps were shown in Figure 5(a) and (b) respectively.

We could find that the effects of bonding layer had limited influence on thermal dissipation. The max temperature of system with SAC305 was only 0.9 degree lower than that with sintered silver. And the max temperature at the end of simulation showed the similar results. In order to evaluate the metallization effects on thermal distribution, we compared the max temperature of sintered Ag-Cu metallization and sintered Ag-Ag metallization systems. The maximum temperatures of Ag-Cu and Ag-Ag system were 161.03 ℃and 161.17 ℃respectively. The results showed that the metallization had less effect on thermal dissipation properties. Therefore, in following parts, we mainly discussed the mechanical simulation results.

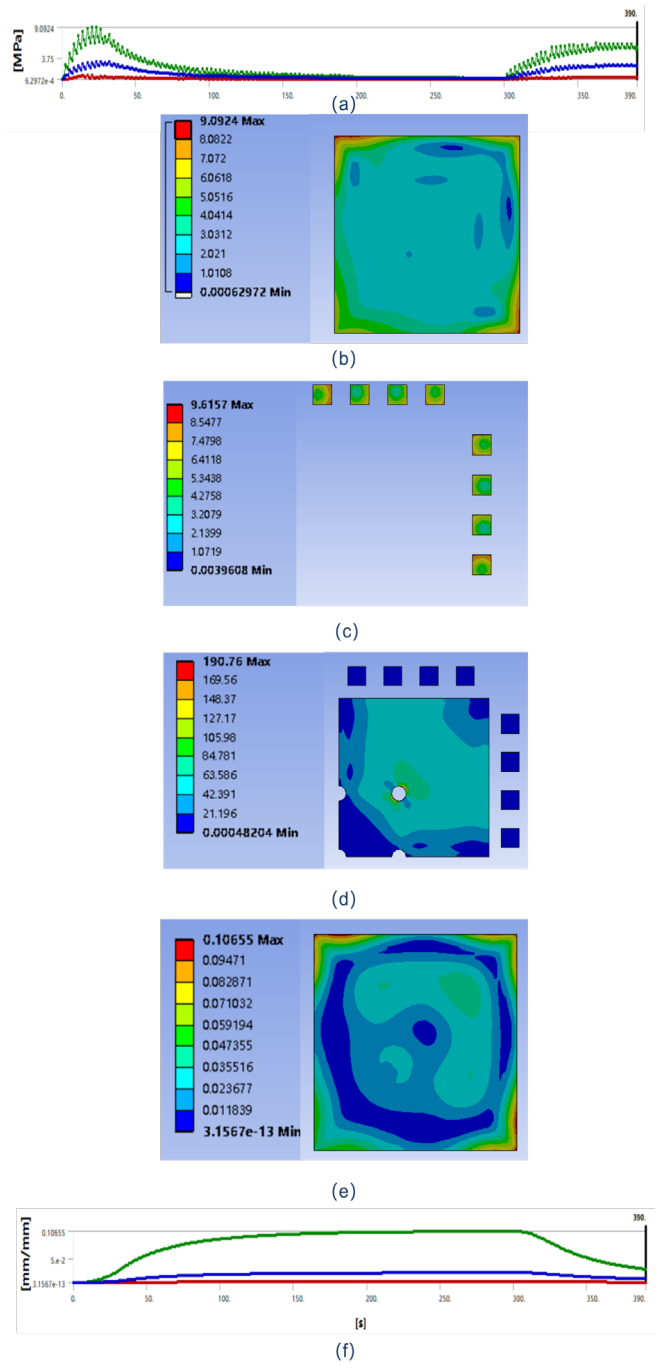

Fig. 6 (a) The stress evolution of bonding layer (b), (c) and (d) were the stress distribution of bonding layer, solders and metallization layer at 20s, (e) was the plastic strain evolution of bonding layer and (f) was the strain evolution of bonding layer at 20s.

B. *Mechanical Analysis*

In this part, we only focus on the stress distribution of joints instead of the whole model. Therefore, we did not analyze the stress state of chip, EMC parts and Cu pad, though the place with maximum stress was around the chips. Since the Anand model of sintered Cu was still in beta stage, the Accuracy of sintered Cu may not higher enough. Therefore, we only used Sintered Ag and SAC305 bonding materials to evaluate the difference between sintered nanomaterials and conventional SAC series material. We first analyzed the thermal behaviors of the system used SAC305 and Cu metallization.

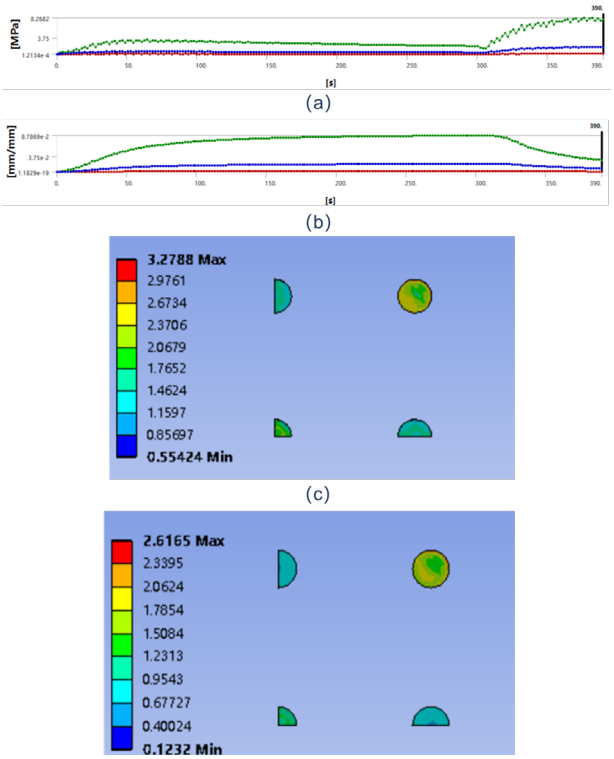

Fig. 7 (a) Stress evolution and (b) plastic strain evolution of bonding layer. (c) and (d) were the stress distribution on vias' filler of SAC305 and sintered Ag

Figure 6(a) was the stress evolution of bonding layer. It was observed that the maximum stress was occurred at 20 s, however the system reached highest temperature at 300℃. After 20s, the stress of bonding layer approximately equaled to 0 with the elevating temperature. And as system cooling down, the stress increased with the decrease the temperature. Figure 6(b), (c), (d) showed the stress distribution of bonding layer, solder and metallization layer at 20s. The max stresses in bonding layer and soler were found at the upleft and downright corner. However, due to the exhibit of via on the metallization, there was stress concentration around the via, which was almost 20 times larger than bonding layer or solder. The max stress of soler was a little higher than that in bonding layer. The max stress place did not change with the temperature evolution, and we did not show the snapshots of stress distribution at other time. And Figure 6(e) was the plastic strain of bonding layer at 300s. Combine the plastic strain evolution curve, we deduced that the reduction of stress after 20s was caused by the large plastic strain. In real experiments, the SAC305 can be

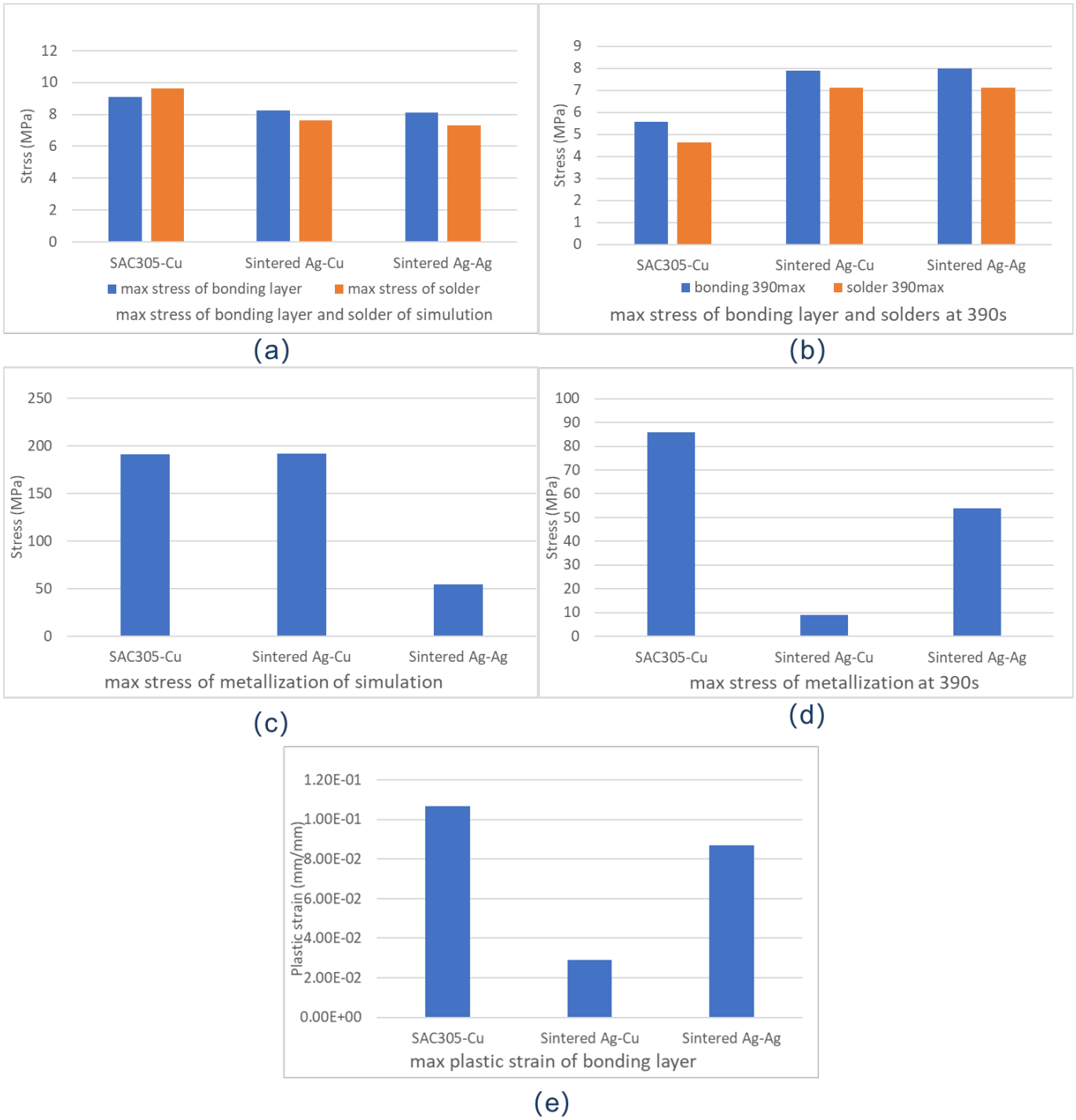

Fig. 8. The bar chart of (a) max stress of bonding layer and solders of the whole simulation, and (b) that of at 390 s, (c) the max stress of metallization of simulation and (d) that of at 390 s, (e) the max plastic strain of bonding layer.

melted at 220 ℃, while the 160 ℃ can make the SAC305 deformation easily under a small force. Figure 1 (a) The stress evolution of bonding layer (b), (c) and (d) were the stress distribution of bonding layer, solders and metallization layer at 20s, (e) was the plastic strain evolution of bonding layer and (f) was the strain evolution of bonding layer at 20s.

However, after 300s, the temperature of system was cooling down, the stress increased again. The reason was that the bonding layer occurred large plastic deformation. Therefore, when the system return to room temperature, the plastic was hard to recover to initial stage. And since the deformation of metallization of Ag at heating stage was elastic strain, as the thermal force decrease, the deformation of metallization could recover to initial state. Mismatches of deformation during cooling and the weakening of SAC's plastic deformation capacity led to an increase in thermal stress.

In order to investigate the material effect, we used the sintered Ag to make a comparison with SAC305 under a same system (the same metallization). Figure 7(a) showed the stress evolution of sintered Ag layer. The stress evolution of sintered Ag was not same the same with that of SAC305, the bonding layer of sintered layer reached to 3.75MPa at around 30 s, which was 2 times smaller than SAC305. After that, the stress of sintered Ag decreased

slowly because of plastic deformation. Both Figure 7(b) and the amplitude of stress evolution showed that the sintered Ag was harder to occur plastic deformation than SAC305 at high temperature. However, the stress rapidly increase of sintered Ag at cooling stage reflected that the utilized of sintered Ag still suffered the problem that the thermomechanical stress generated during cooling stage. And the curves showed that there were larger stress generated at cooling stage. This results can be contributed by the SAC305 was easier to generate plastic deformation than sintered Ag. Therefore, the material deformation of mismatch of thermal expansion can transformed to plastic strain instead of a large part of elastic strain. According to compare the plastic strain of sintered Ag with 0.06, the plastic strain of SAC almost reached to 0.08.

We should illustrate that although bonding material was not only used for bonding layer and solders, but also used to fill the vias. However, since the bonding materials in the via was significantly smaller than bonding layer and solders as shown in figure 7 (c) and (d), we did not discuss the behavior of vias' filler.

In previous parts we only exhibit the stress and plastic strain evolution and stress distribution, and we did not compare the key results quantity. Therefore, we showed the maximum stress or plastic strain of the whole simulation and specific time as shown in Figure 8. In order to save article space, we also put the Sintered Ag-Ag metallization results in Figure 8, which was used to illustrate the metallization effects in next part.

Figure 2 The bar chart of (a) max stress of bonding layer and solders of the whole simulation, and (b) that of at 390 s, (c) the max stress of metallization of simulation and (d) that of at 390 s, (e) the max plastic strain of bonding layer.

The results showed that the max thermal stress of SAC305 was a little higher than that of sintered Ag. However, the time point that presented the max stress was different. The max stress in SAC305 occurred at the beginning of heating process, while the max stress in sintered Ag was occurred at the end of the simulation as shown in figure 8(b). At the end of the simulation, the stress of sintered Ag was almost 3 MPa larger than SAC305. However, to our surprise, the max stress of metallization of the system of both SAC305 and sintered Ag were the same. This means that the bonding materials had less effect on the stress of metallization. As the temperature was cooling down, the stress of metallization decreased with different degrees. The SAC305 decreased to 85 MPa and sintered Ag decreased to 8 MPa, which was only one-tenth the stress of SAC305. This results showed that the sintered Ag generated less force after a power cycling test, which means that the sintered Ag had better reliability than that of SAC 305. The underlying reasons of this results was that there was larger plastic strain generated during the heating process, which was the irreversible behaviors. In terms of sintered Ag, the bonding layer or solders had less plastic strain as shown in figure 8(e). Therefore, the stress caused by the mismatch of CTE can only induce the elastic strain in sintered Ag. As the thermal stress decrease during the cooling down process, the strain could recover rapidly.

The metallization could also effect the stress state in the junction as shown in Figure 8. We could find that the max stress of sintering had little variation under the change of metallization in the whole simulation. However, we found that the max stress of Ag metallization was much smaller than that of Cu metallization as shown in figure 8(c). The max stress of Ag metallization reduced to 25% of that of Ag metallization. We attributed this results to the plastic deformation in bonding layer as shown in figure 8 (e). This also caused the stress of Ag bonding layer a little larger than that of Cu bonding layer at 390s.And as the temperature decrease, the decrease of stress amplitude of Ag metallization was not significantly as that of Cu metallization. Therefore, the variation of metallization from Cu to Ag had different performance at different stage of thermal/power cycling. During the heating process, the utilized of Ag metallization could avoid the larger stress generated around the vias. Due to the plastic strain of bonding layer in system with Ag metallization, as the temperature decreased after heating process, the thermal stress of Ag metallization was higher than that of Cu metallization. Hence, the utilized of Ag could significantly reduce stress during heating process, while this strategy can also cause the higher thermal stress at low temperature. This may result in a worse reliability than system used Cu metallization.

IV. Conclusion

In this paper, we investigated the bonding materials and metallization effects on thermal and mechanical properties of GaN based QFN Package. The results showed that the SAC305 and sintered Ag had little effects on thermal distribution, although the thermal conductivities of SAC was much lower than that of sintered Ag. The selection of metallization materials also had little effects on thermal conductivity. However, the bonding materials and metallization had significant effects on stress state of junction. As SAC305 was much easier generated plastic deformation at high temperatures, which was not benefit for power electronic devices because of extra deformation and stress during cooling process. In terms of sintered Ag, the bonding layer generated more elastic strain. As the deformation recovered to initial stage, the stress decreased because of the elastic strain. And we also found that the Ag metallization could decreased the maximum stress of model at heating stage. But Ag metallization suffered larger thermal stress as the temperature decreased.

[1] B. Ji, X. Song, E. Sciberras, W. Cao, Y. Hu, and V. Pickert, "Multiobjective Design Optimization of IGBT Power Modules Considering Power Cycling and Thermal Cycling," *IEEE Transactions on Power Electronics*, vol. 30, no. 5, pp. 2493–2504, May 2015, doi: 10.1109/TPEL.2014.2365531.

[2] F. Iacopi, M. Van Hove, M. Charles, and K. Endo, "Power electronics with wide bandgap materials: Toward greener, more efficient technologies," *MRS Bull.*, vol. 40, no. 5, pp. 390–395, May 2015, doi: 10.1557/mrs.2015.71.

[3] J. G. Kassakian and T. M. Jahns, "Evolving and Emerging Applications of Power Electronics in Systems," *IEEE Journal of Emerging and Selected Topics in Power Electronics*, vol. 1, no. 2, pp. 47–58, Jun. 2013, doi: 10.1109/JESTPE.2013.2271111.

[4] R. Khazaka, L. Mendizabal, D. Henry, and R. Hanna, "Survey of High-Temperature Reliability of Power Electronics Packaging Components," *IEEE Transactions on Power Electronics*, vol. 30, no. 5, pp. 2456–2464, May 2015, doi: 10.1109/TPEL.2014.2357836.

[5] L. A. Navarro *et al.*, "Thermomechanical Assessment of Die-Attach Materials for Wide Bandgap Semiconductor Devices and Harsh Environment Applications," *IEEE Transactions on Power*

Electronics, vol. 29, no. 5, pp. 2261–2271, May 2014, doi: 10.1109/TPEL.2013.2279607.

[6] C. Hang, J. He, Z. Zhang, H. Chen, and M. Li, "Low Temperature Bonding by Infiltrating Sn3.5Ag Solder into Porous Ag Sheet for High Temperature Die Attachment in Power Device Packaging," *Sci Rep*, vol. 8, no. 1, p. 17422, Dec. 2018, doi: 10.1038/s41598-018-35708-6.

[7] K. Hollstein, X. Yang, and K. Weide-Zaage, "Thermal analysis of the design parameters of a QFN package soldered on a PCB using a simulation approach," *Microelectronics Reliability*, vol. 120, p. 114118, May 2021, doi: 10.1016/j.microrel.2021.114118.

[8] J. H. Lau, "State of the Art of Lead-Free Solder Joint Reliability," *Journal of Electronic Packaging*, vol. 143, no. 2, p. 020803, Jun. 2021, doi: 10.1115/1.4048037.